Supplement of Atmos. Meas. Tech., 12, 1365–1373, 2019
https://doi.org/10.5194/amt-12-1365-2019-supplement

Atmospheric Measurement Techniques
Open Access
EGU

Supplement of

Aerosol light absorption from optical measurements of PTFE membrane filter samples: sensitivity analysis of optical depth measures

A. Pandey et al.

Correspondence to: Rajan K. Chakrabarty (chakrabarty@wustl.edu)

Supplement of

Aerosol light absorption from attenuation measurements of PTFE-membrane filter samples: sensitivity analysis of optical depth measures

Apoorva Pandey[1], Nishit J. Shetty[1], and Rajan K. Chakrabarty[1,2]
[1]Center for Aerosol Science and Engineering, Department of Energy, Environmental and Chemical Engineering, Washington University in St. Louis, St. Louis, MO 63130, USA
[2]McDonnell Center for the Space Sciences, Washington University in St. Louis, St. Louis, MO 63130, USA

S1. Experimental methods

Fuel types and combustion conditions, with corresponding single scattering albedo (SSA) values and absorption Ångström exponents (AÅE), are listed in Table 1 in the manuscript. Burn protocols for the three combustion phases were as follows:

1) Peat was smoldered using a heating plate at a temperature of 200□ C. Other biomass types were smoldered by first establishing flaming (for 1-2 min) by igniting the fuel with a lighter and then starving the flame by covering the fuel container. While the biomass was flaming, the chamber exhaust was left open; the exhaust was closed once the flames were extinguished. The sample line between the chamber and mixing volume was connected 5 min after closing the exhaust.
2) To isolate the flaming phase, the biomass was ignited with a lighter and the chamber exhaust was closed. We monitored the flame visually from outside the combustion chamber, closing off the sample line between the chamber and the mixing volume once the flames were out.
3) For mixed phase sampling, flaming was established following the procedure above and emissions were continuously pulled into the mixing volume even after the flames were extinguished.

Some biomass types like Ponderosa pine and Douglas fir did not sustain smoldering combustion and were only sampled in flaming and mixed conditions. Other types like dung and Lodgepole pine were found to not sustain a flame. Kerosene was burned using a wick lamp. Intrinsic optical properties from the combustion of certain biomass types varied from burn to burn for the same combustion protocol. For such cases, the ranges of observed properties are given in the table below. During each burn, a steady state (10-40 min long) was established within which the absorption and scattering coefficients were nearly constant.

S2. Two-stream radiative transfer model

Consider the layer of filter in which sampled particles are embedded to be a one-dimensional uniform medium with an optical thickness τ_0, a single scattering albedo $\omega<1$ and a scattering asymmetry parameter g. Now, consider a 'forward' direction: at any point in the medium the energy intensity propagating in this direction is given by I_f. Conversely, the backward propagation intensity is I_b.

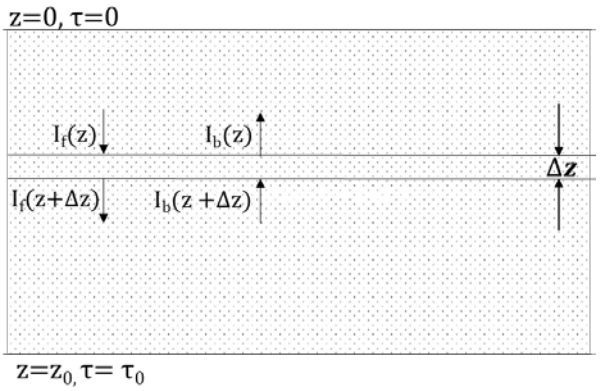

Figure S1: Transmission and reflection of radiation through a one-dimensional, uniformly multiple-scattering medium.

Energy conservation in the medium can be written as(Bohren, 1987):

$$\frac{d(I_f - I_b)}{d\tau} = -(1-\omega_0)(I_f + I_b) \quad \text{(S1a)}$$

$$\frac{d(I_f + I_b)}{d\tau} = -(1-\omega_0 g))(I_f - I_b) \quad \text{(S1b)}$$

The general solution of the above equations has the following form:

$$(I_f - I_b) = p_1 \exp(-K\tau) + p_2 \exp(K\tau) \quad \text{(S2a)}$$

$$(I_f + I_b) = q_1 \exp(-K\tau) + q_2 \exp(K\tau) \quad \text{(S2b)}$$

where $K = \sqrt{(1-\omega_0)(1-\omega_0 g)}$

Assume that the medium is (1) illuminated from the top: $I_f(\tau = 0) = I_0$ and (2) does not reflect at the opposite edge: $I_b(\tau = \tau_0) = 0$. Reflectance R_l and transmittance T_l of the medium are respectively defined as: $I_b(\tau = 0) = R_l$ and $I_f(\tau = \tau_0) = T_l$. With these boundary conditions, the constants p_1, p_2, q_1 and q_2 can be estimated. Then the quantities of interest, R_l and T_l, are given by(Arnott et al., 2005):

$$R_l = \frac{\omega_0(1-g)\,sinh(K\tau_0)}{[2K - \omega_0(1-g)\,sinh(K\tau_0) + 2K\,cosh(K\tau_0)]} \quad \text{(S3a)}$$

$$T_l = \frac{2}{[2K - \omega_0(1-g)\,sinh(K\tau_0) + 2K\,cosh(K\tau_0)]} \quad \text{(S3b)}$$

Note that in the manuscript the subscript *l* is used in the equations above to denote the properties of a composite aerosol-filter layer. τ_0 denotes the total optical depth of the layer:

$$\tau_0 = \tau_{e,l} = \tau_{e,f+}\,\tau_{a,s} + \tau_{sc,s} \quad \text{(S4)}$$

Subscripts *e, a* and *sc* denote extinction, absorption and scattering optical depths. The second subscript *f* corresponds to the portion of the filter that was penetrated by the aerosol, while *s* represents the aerosol sample. Eq. (4) can be rewritten as:

$$\tau_{e,l} = \chi\tau_{e,F+}\,\tau_{a,s}\left(\frac{1+SSA}{1-SSA}\right) \quad \text{(S5)}$$

where χ is the penetration depth of the aerosols in the filter (assumed 0.1 in this study). A two-layer schematic of the filter with a given aerosol penetration depth is showed in Fig. S2. The optical depth of the filter in the first layer is proportional to the penetration depth and the optical depth of a blank filter, $\tau_{e.F.}$ In eq. S5, SSA is the single scattering albedo of the deposited aerosols. The single scattering albedo and asymmetry parameter of this composite layer are given by:

$$\omega_0 = \frac{\tau_{a,s}\left(\frac{SSA}{1-SSA}\right)+\chi\tau_{e,F}}{\tau_{a,s}\left(\frac{1+SSA}{1-SSA}\right)+\chi\tau_{e,F}} \quad \text{(S6)}$$

$$g = \frac{g_S \times \tau_{a,s}\left(\frac{SSA}{1-SSA}\right)+g_F \times \chi\tau_{e,F}}{\tau_{a,s}\left(\frac{SSA}{1-SSA}\right)+\chi\tau_{e,F}} \quad \text{(S7)}$$

The respective asymmetry parameters of the particles and filter are denoted by g_s and g_F. In this study, was g_s fixed at 0.6 (based on Martins et al. (1998); Reid et al. (2005)).

For the pristine portion of the filter (no aerosol embedded, therefore single scattering albedo is unity), the solution to Eq.s (S1a) and (S1b) is greatly simplified. The reflectance (*R2*) and transmittance (*T2*) of this layer is given by:

$$R_f = \frac{(1-\chi)\tau_F^*}{1+(1-\chi)\tau_F^*} \quad \text{(S8a)}$$

$$T_f = \frac{1}{1+(1-\chi)\tau_F^*} \quad \text{(S8b)}$$

where $\tau_F^* = \left(1 - g_F\right)\tau_F$ is estimated from the measurements of transmittance and reflectance through blank filters. Since a blank filter is non-absorbing, Eq.s (S8a) and (S8b) can be applied to it, setting χ as zero (i.e. no loading). Measured transmittance through 20 lab blank PTFE membrane filters for wavelengths ranging 350-550 nm was 0.7±0.02. This range (2 standard deviations are ~6% around the mean) is slightly narrower than that (~10%) observed by White et al., 2016 for 534 passively exposed field blanks from the IMPROVE network. It is comparable to the variability in transmittance (~7%) of 150 clean blanks reported by Presler-Jur, 2017.

For T_{blank}=0.7, τ^*_F is calculated as:

$$\tau_F^* = \frac{1}{T_{blank}} - 1 = 0.43 \quad \text{(S9)}$$

This value of τ^*_F was used in the fixed blank optics assumption (Fig.s 2 and 5 in the main manuscript and Fig.s S2-S4) when examining the sensitivity to filter optical measures to a given model input. Some calculations were also performed assuming a realistic range of randomly-varying blank filter properties, as in Fig. 3 in the manuscript and Fig. S5 below.

It can be shown that all calculations in equations S3a through S8b require only τ^*_F and not τ_F and g_F. Therefore, any non-zero value can be assumed for τ_F and g_F can be calculated such that the value of τ^*_F is satisfied. With these filter properties (τ_F and g_F), and assumed aerosol penetration depth χ (see Fig. S3 for sensitivity of model outputs to this parameter) and asymmetry parameter g_s, R_l, R_f, T_l and T_f were calculated for a range of aerosol properties ($\tau_{a,s}$ and SSA). Then, overall filter transmittance and reflectance, with light incident on the sample side of the filter, were estimated by performing an energy balance(Gorbunov et al., 2002):

$$T_s = \frac{T_l T_f}{1 - R_l R_f} \tag{S10A}$$

$$R_s = R_l + \frac{T_l^2 R_f}{1 - R_l R_f} \tag{S10B}$$

The optical behavior of PTFE filters was modeled for SSA varied between 0.2 and 0.99, and $\tau_{a,s}$ between 0 and 1. In Fig. S2, the change in R_s with respect to R_b is plotted against the associated change in T_s, with increasing filter loading, for two discrete SSA values. For large values of SSA (>0.85), R_s is predicted to be larger than R_b, while for smaller SSA, R_s decreases with increasing loading and remains smaller than R_b. These findings hold for varying assumed values of the penetration depth (χ), as shown in Fig. S3.

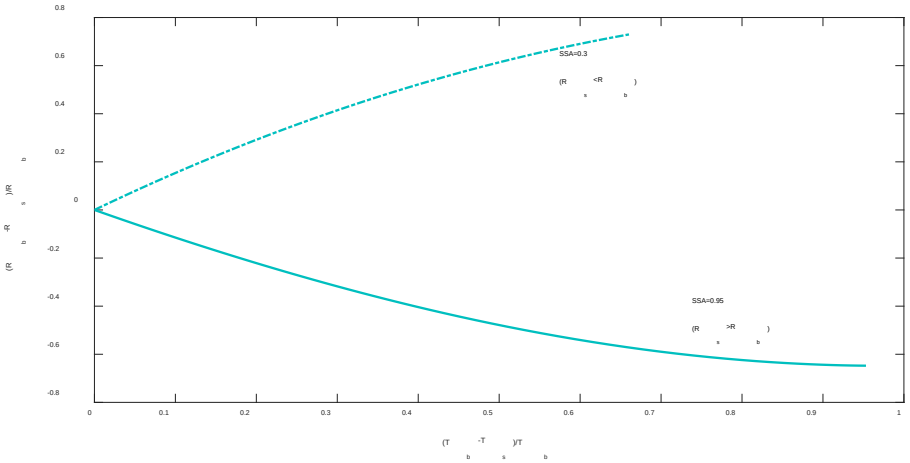

Figure S2: Change in sample-side reflectance as a function of the corresponding change in transmittance for predominantly absorbing (SSA=0.3) and scattering (SSA=0.95) aerosol types when blank optics are fixed.

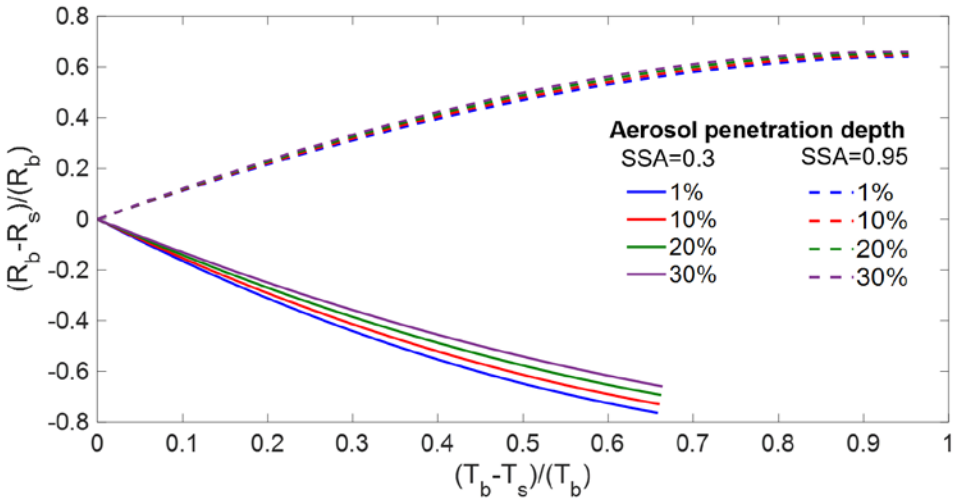

Figure S3: Same as Fig. S2 but for different assumed values of aerosol penetration depth χ.

Fig. S4 shows the variation of $OD_S = \ln(\frac{1-R_S}{T_S})$ over the input ranges of SSA and $\tau_{a,s}$.

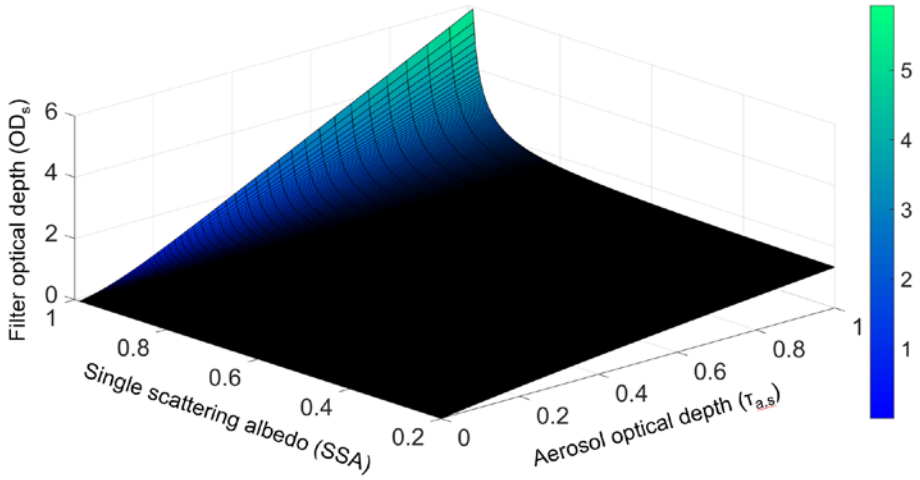

Figure S4: Modeled filter optical depth (OD_s) as a function of single scattering albedo (SSA) and aerosol optical depth ($\tau_{a,s}$) of deposited aerosols.

The above R_s and T_s calculations were also applied to experimentally observed values of $\tau_{a,s}$ and SSA (Fig. S5). The three measures of filter optical depth defined in the manuscript are plotted against the *in-situ* aerosol optical depths associated with each sample. Overall, OD_c is closer to the actual aerosol optical depth $\tau_{a,s}$ than *ODs*. However, OD_s shows a slightly stronger correlation with $\tau_{a,s}$ (R^2=0.99, least-squares power law fit $y=0.61*x^{1.08}$) than OD_c (R^2=0.97, $y=0.73*x^{0.93}$).

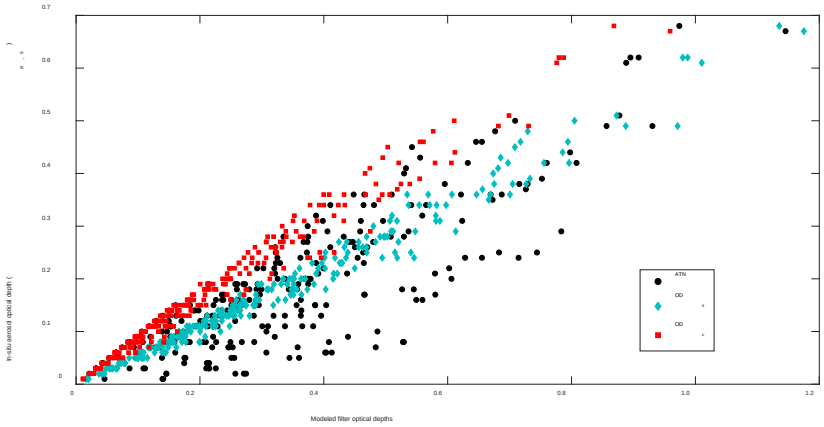

Figure S5: The relationship between experimentally measured *in-situ* aerosol optical depth ($\tau_{a,s}$) and modeled values of filter optical depth measures (OD_c, ATN and OD_s). Blank optics were randomly generated for each sample point from a normal distribution with mean=0.7 and standard deviation=0.02.

S3. Filter correction factor *C*

Fig. S6 shows the filter correction factor *C* plotted against filter optical loading (attenuation) and the aerosol single scattering albedo. As the correction factor was calculated by dividing the absorption optical depth of the deposited aerosols by the attenuation through the corresponding filter sample, uncertainties in the correction factor contain experimental errors from both measurements. This combined error, as well as the mathematical nature of the relationship between absorption optical depth and attenuation, leads to difficulty in fitting a curve to the data in Fig. S6A. No correlation was found between the correction factor and attenuation datasets.

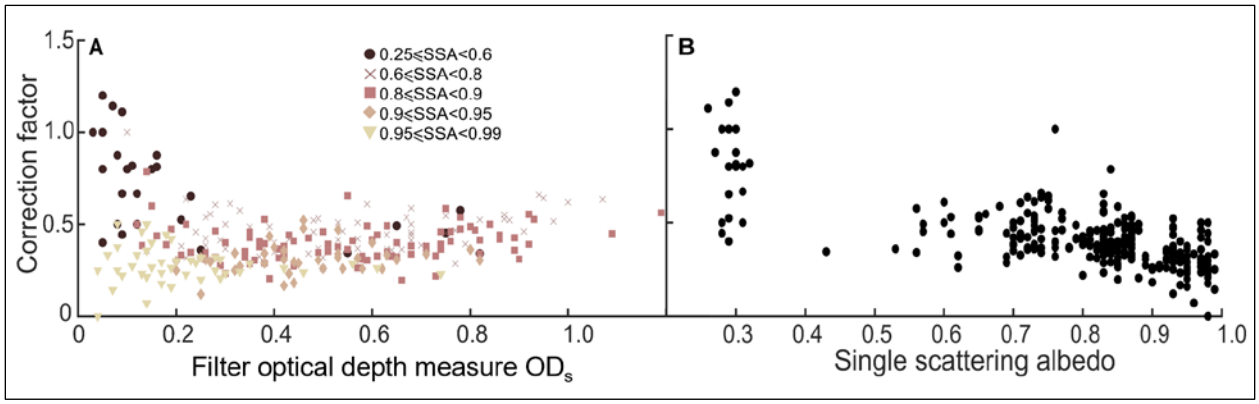

Figure S6: Correction factor *C* (ratio of $\tau_{a,s}$ to OD_s) as a function of A) filter optical depth OD_s and B) single scattering albedo of the deposited particles.

References

Arnott, W. P., Hamasha, K., Moosmüller, H., Sheridan, P. J., and Ogren, J. A.: Towards aerosol light-absorption measurements with a 7-wavelength aethalometer: Evaluation with a photoacoustic instrument and 3-wavelength nephelometer, Aerosol Science and Technology, 39, 17-29, 2005.

Bohren, C. F.: Multiple scattering of light and some of its observable consequences, Am. J. Phys, 55, 524-533, 1987.

Bond, T. C., Doherty, S. J., Fahey, D., Forster, P., Berntsen, T., DeAngelo, B., Flanner, M., Ghan, S., Kärcher, B., and Koch, D.: Bounding the role of black carbon in the climate system: A scientific assessment, Journal of Geophysical Research: Atmospheres, 118, 5380-5552, 2013.

Gorbunov, B., Hamilton, R., and Hitzenberger, R.: Modeling radiative transfer by aerosol particles on a filter, Aerosol Science & Technology, 36, 123-135, 2002.

Martins, J. V., Artaxo, P., Liousse, C., Reid, J. S., Hobbs, P. V., and Kaufman, Y. J.: Effects of black carbon content, particle size, and mixing on light absorption by aerosols from biomass burning in Brazil, Journal of Geophysical Research: Atmospheres, 103, 32041-32050, 1998.

Reid, J., Koppmann, R., Eck, T., and Eleuterio, D.: A review of biomass burning emissions part II: intensive physical properties of biomass burning particles, Atmos. Chem. Phys., 5, 799-825, 2005.

Presler-Jur, P., Doraiswamy, P., Hammond, O., & Rice, J.: An evaluation of mass absorption cross-section for optical carbon analysis on Teflon filter media. Journal of the Air & Waste Management Association, 67(11), 1213-1228, 2017.

White, W. H., Trzepla, K., Hyslop, N. P., and Schichtel, B. A.: A critical review of filter transmittance measurements for aerosol light absorption, and de novo calibration for a decade of monitoring on PTFE membranes, Aerosol Science and Technology, 50, 984-1002, 2016.